Stem Cell Reports, Volume *17*

Supplemental Information

Characterizing arrhythmia using machine learning analysis of Ca^{2+} cycling in human cardiomyocytes

Jeremy K.S. Pang, Sabrina Chia, Jinqiu Zhang, Piotr Szyniarowski, Colin Stewart, Henry Yang, Woon-Khiong Chan, Shi Yan Ng, and Boon-Seng Soh

Supplemental Materials

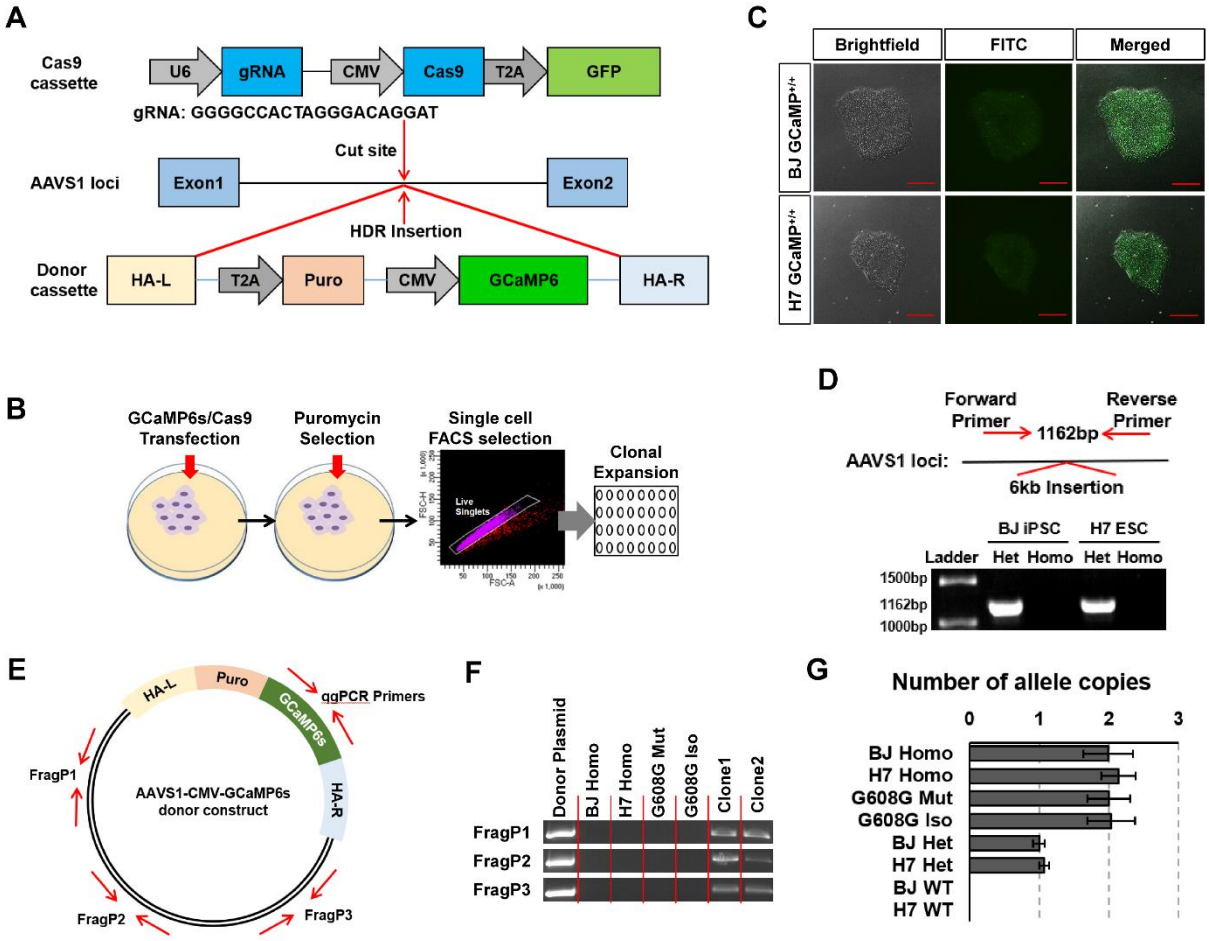

Figure S1: Related to Figure 2A for homozygous knock-in of GCaMP6s into hPSC lines
(A) Schematic representing the CRISPR-Cas9 strategy to insert the GCaMP6s sequence into the AAVS1 loci. **(B)** Efficient clonal isolation with successful insertions was achieved by puromycin selection followed by fluorescence activated cell sorting of single cells into individual wells. **(C)** Representative fluorescence images of hPSC clones with successful insertions. Constitutive GCaMP6s expression results in faint fluorescence in hPSCs observable under FITC filters. Scale bar = 200µm **(D)** Homozygous GCaMP6s insertion is confirmed using gel electrophoresis genotyping for the complete loss of the 1162bp amplicon spanning the insertion site. **(E)** Plasmid map denoting the primers used to PCR for plasmid fragments and the qgPCR primers used for allele copy number quantitative genotyping PCR. **(F)** PCR analysis for plasmid fragments of the GCaMP6s donor plasmid outside of the insertion cassette. Donor plasmid DNA was amplified as an amplification control (Lane 1). Clone1 and Clone2 were two positive control clones found to contain plasmid fragments (Lane 6 and 7). **(G)** GCaMP6s allele copy number quantitative genotyping PCR for the four parental lines used in this work (H7 Homo, BJ Homo, G608G Mut, G608G Iso), together with two heterozygous clones and the two WT hPSC lines. CT values were normalized to RELL2 as a stable housekeeping gene corresponding to 2 allele copies of a gene. ΔCT values were normalized to BJ Het to obtain ΔΔCT values corresponding to the number of allele copies of GCaMP6s insertions. Data is represented as Fold Change ± SD (N = 3 technical replicates). BJ WT and H7 WT were undetected at a threshold of 40 cycles. **Het,** Heterozygous; **Homo,** Homozygous.

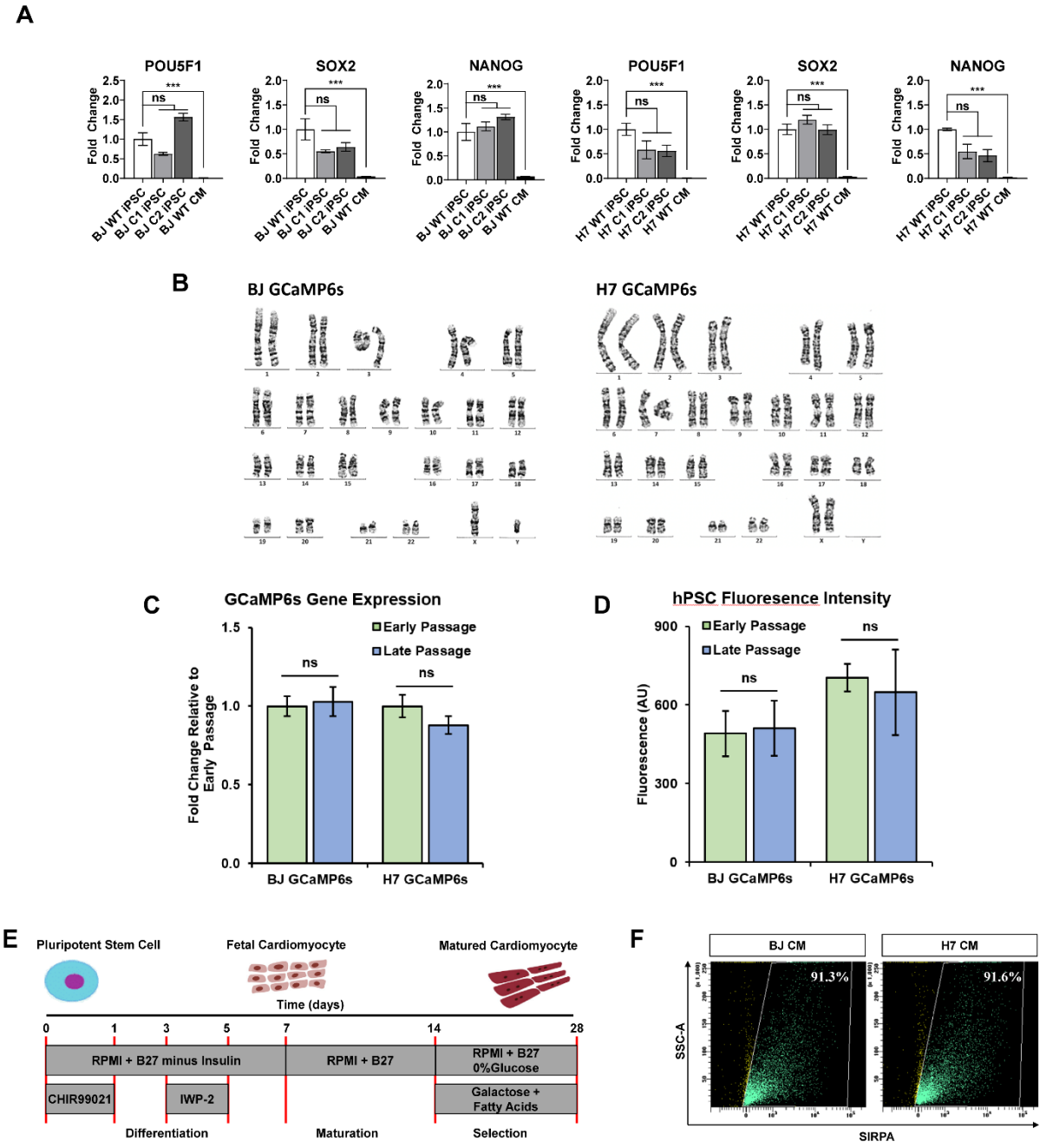

Figure S2: Related to Figure 2A for validation of successful generation of GCaMP6s expressing hPSC-CMs

(A) Quantitation of pluripotency gene expression levels for changes due to GCaMP6s insertion. Non-significant changes in both C1 (Heterozygous) and C2 (Homozygous) GCaMP6s insertions into BJ iPSCs (Left) or H7 ESCs (Right) confirms maintenance of pluripotency state. Comparison with differentiated CMs was included to highlight expected reduction in pluripotency gene expression when hPSCs leave the pluripotency state. *N* = 3 biological replicates; Mean ± SD are plotted. *ACTB* is used as the housekeeping gene. Asterisks indicate statistical significance (***P<0.001; ns, P>0.05; two-tailed Students *t* test). **(B)** Karyotyping analysis for BJ GCaMP6s (Left) and H7 GCaMP6s (Right) lines. **(C)** Quantitative PCR comparison of GCaMP6s expression between Early (Passage <10) and Late (Passage ~30) passage hPSCs post clonal isolation. *N* = 3 biological replicates; Mean ± SD are plotted. *ACTB* is used as the housekeeping gene. Asterisks indicate statistical significance (ns, P>0.05; two-tailed Students *t* test). **(D)** Fluorescence intensity quantification for hPSC lines in Early and Late passages post GCaMP6s insertion and clonal isolation. *N* = 67 colonies (BJ Lines) and *N* = 26 colonies (H7 Lines). **(E)** Directed CM differentiation and maturation protocol. **(F)** Representative flow cytometric analysis of Day 28 hPSC-CM representing matured, enriched CM populations.

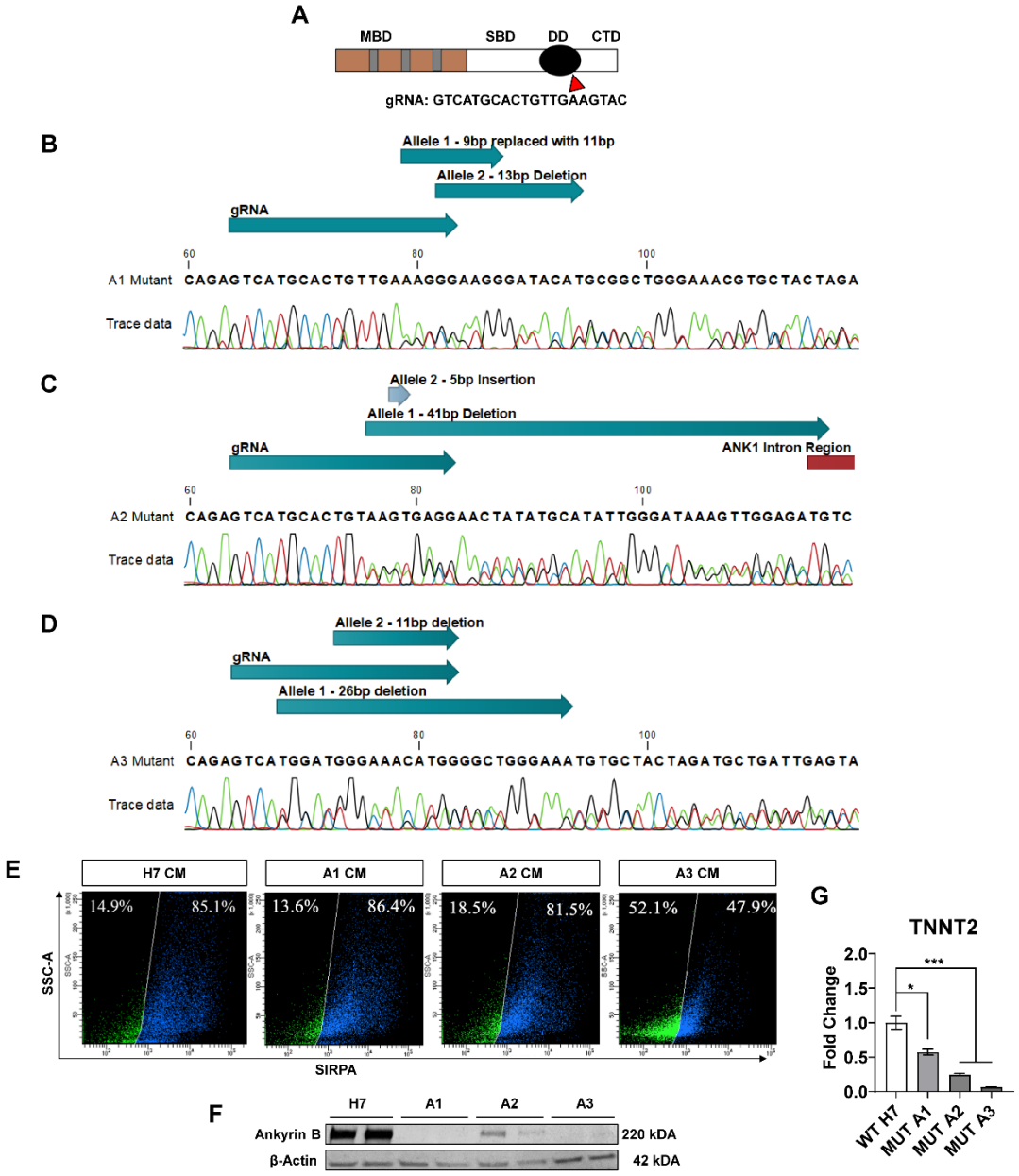

Figure S3: Related to Figure 3A for the characterising of AnkB mutant clones
(A) Schematic depicting the gRNA used to target Exon 40 of *ANK2* locus coding for the death domain of AnkB. Polymorphic mutations in the death domain and the C-Terminus domain have been linked with genetic dispositions to arrhythmias. **MBD**, Multiple Binding Domain; **SBD**, Spectrin Binding Domain; **DD**, Death Domain; **CTD**, C-Terminus Domain. **(B** to **D)**, Sequencing data of the *ANK2* locus targeted by the gRNA for A1, A2 and A3 mutant lines respectively. For all three cell lines, biallelic frameshifts are expected. For A2 mutant, the 41bp Allele 1 deletion cuts into the following intronic region by 2 base pairs. Therefore, a 39bp deletion in-frame deletion of Exon 40 is expected, with a potential deletion of the splice domain. Exact insertion and deletion sequences are listed in Table S5. **(E)** Representative flow cytometry analysis of day 14 hESC-CMs before metabolic selection was done. **(F)** Western blot for AnkB protein expression in H7, A1, A2 and A3 day 28 hESC-CMs. Homozygous knock-outs are confirmed in A1 and A3 mutants, while heterozygous knock-out is confirmed in A2 mutant. **(G)** Quantitation of cardiomyocyte marker *TNNT2* expression levels showed significant reduction in expression for all three mutants confirming the poorer differentiation efficiency and maturation capabilities of the mutant CMs. *N* = 3 biological replicates; Mean ± SD are plotted. *ACTB* is used as the housekeeping gene. Asterisks indicate statistical significance (***P<0.001; *P<0.05; two-tailed Students *t* test).

.

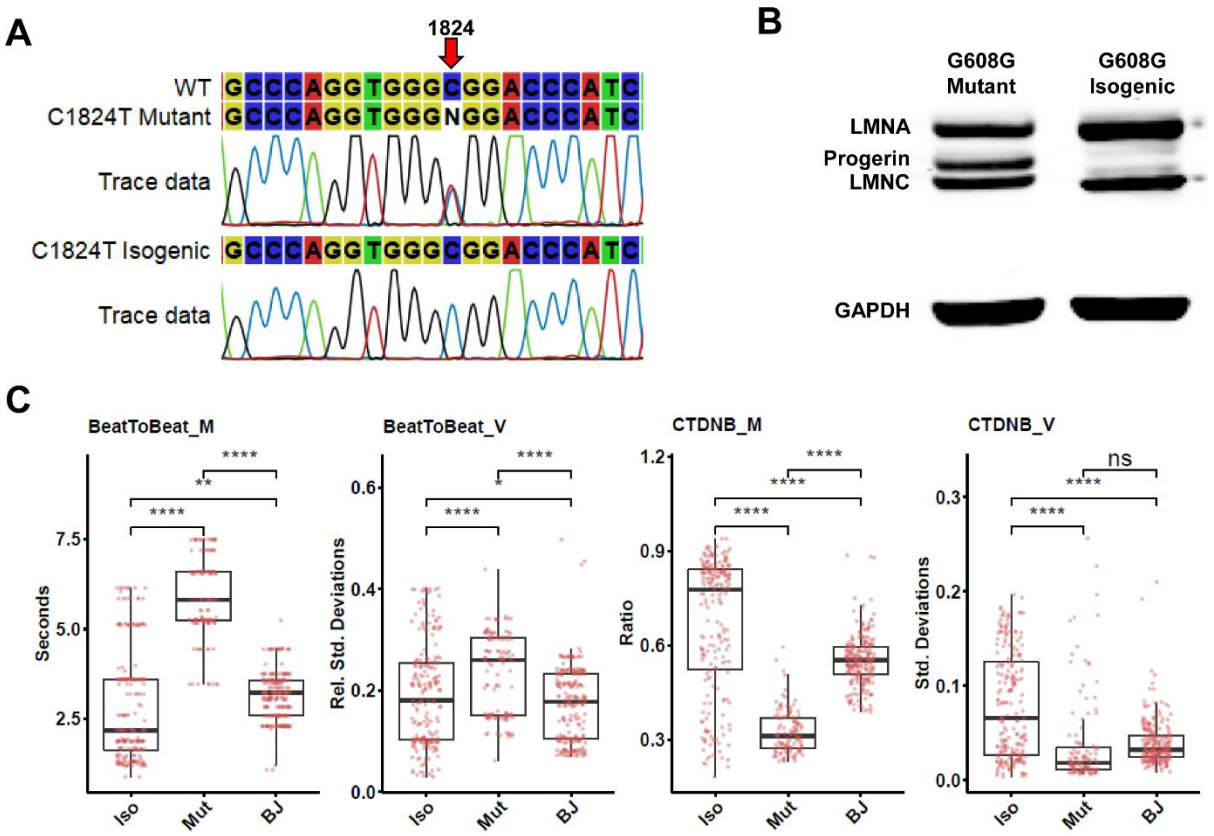

Figure S4: Related to Figure 3A for the characterising the electrophysiology of congenital HGPS mutation

(A) Sequencing confirmation showing C1824T heterozygous mutation present in G608G HGPS mutant iPSC line repaired in the isogenic iPSC line. **(B)** Western blot for Lamin A/C protein expression in the HGPS G608G mutant line and the corrected isogenic control. Correction of the mutation resulted in loss of no Progerin build up. **(C)** Boxplots depicting quantitative comparison across treatment groups for beat to beat duration, mean and standard deviation (BeatToBeat_M and BeatToBeat_V respectively) and CTDNB, mean and standard deviation (CTDNB_M and CTDNB_V respectively). Boxplots represent the median of the data (central line), data between first and third quartiles (box), data within 1.5x of the interquartile range (whiskers) and outliers (points beyond the whiskers). Each point represents a single hPSC-CM. Asterisks indicate statistical significance (****P<0.0001; *P<0.05; two-tailed Students *t* test). **Iso,** Isogenic healthy HGPS-CM, *N* = 211; **Mut,** Progeria HGPS-CM, *N* = 120; **BJ,** Healthy BJ-CM, *N* = 211.

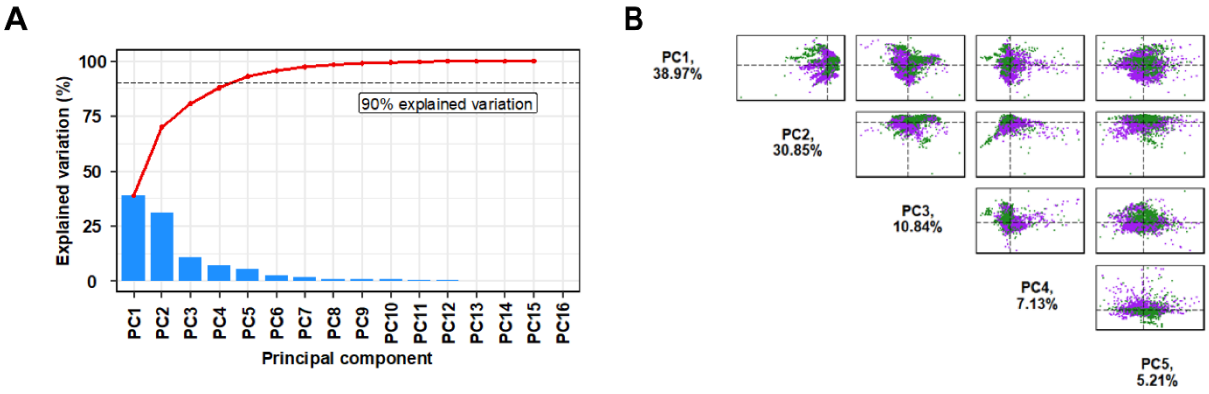

Figure S5: Related to Figure 3B
(A) Scree plot of the PCA shows that the first 5 PCs explains >90% of variation present. **(B)** Pairs plot showing the different combination pairs of the first 5 PCs. No clear distinction between healthy and arrhythmic classes can be observed.

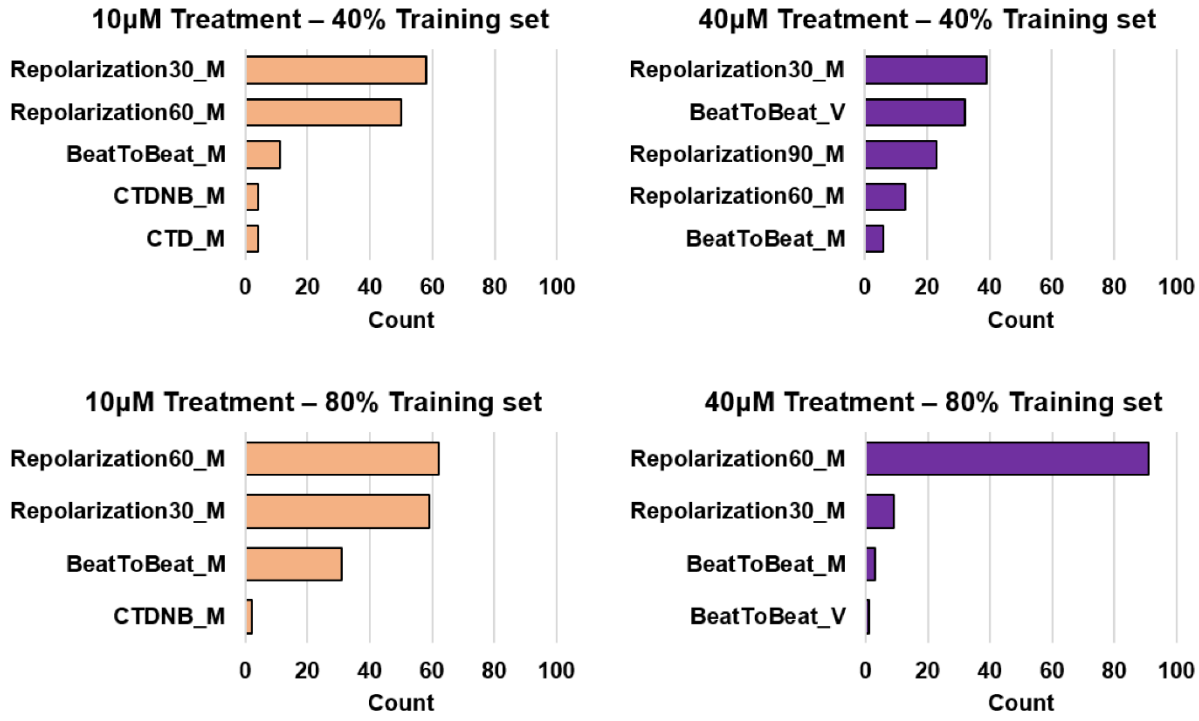

Figure S6: Related to Figure 5
Total count of all parameters that scored >20 on the feature importance metrics across XGB models trained using different train-test splits. **Top**, 40-60 train-test split; **Bottom**, 80-20 train-test split.

Table S1: Related to Results

Mathematical descriptors of individual Ca^{2+} transient parameters for a single contraction. All mathematical notation is defined similarly across different parameters.

Calcium transient parameters	Mathematical descriptor
Beat-To-Beat Duration $\boldsymbol{T_{BTB}}$	$\boldsymbol{T_{BTB,i} = T_{Max,i+1} - T_{Max,a}}$ Where $\boldsymbol{T_{Max,i}}$ is the timestamp of the maximum intensity of a single contraction ***i***
Depolarization Duration $\boldsymbol{T_{DD}}$	$\boldsymbol{T_{DD,i} = T_{Max,i} - T_{Min,i}}$ Where $\boldsymbol{T_{Min,i}}$ is the timestamp of the minimum intensity of contraction ***i***
Repolarization Duration $\boldsymbol{T_{R30\ /\ R60\ /\ R90}}$ For 30%,60%,90% repolarization	$\boldsymbol{T_{R30/R60/R90,i} = T_{Int30/60/90,i} - T_{Max,i}}$ $\boldsymbol{T_{Int30/60/90,i}}$ is the timestamp of 30/60/90% reduction from the maximum intensity of contraction ***i***
Calcium Transient Duration $\boldsymbol{T_{CTD}}$	$\boldsymbol{T_{CTD,i} = T_{Int90,i} - T_{Min,i}}$ Where $\boldsymbol{T_i}$ is the timestamp of contraction ***i***

Table S2: Related to Results

Mathematical descriptors of normalized compound variables for a single contraction.

Compound Variables	Mathematical descriptor
Calcium Transient Duration Normalized to Beat to beat duration ***CTD NB***	$\boldsymbol{CTD\ NB_i = \frac{T_{CTD,i}}{T_{BTB,i}}}$ For a single contraction ***i***
Depolarization Duration Normalized to Calcium Transient Duration ***Depolarization NCTD***	$\boldsymbol{Depolarization\ NCTD_i = \frac{T_{DD,i}}{T_{CTD,i}}}$ For a single contraction ***i***
Repolarization 30% Duration Normalized to Repolarization 90% Duration ***Repolarization30 NR90***	$\boldsymbol{Repolarization30\ NR90_i = \frac{T_{R30,i}}{T_{R90,i}}}$ For a single contraction ***i***

Table S3: Related to Results

Theorized molecular explanations for the mean of each Ca^{2+} handling parameter of an individual cardiomyocyte

Parameter (Means)	**Biological Meaning**
Beat to Beat Duration Mean $\overline{T}_{BTB}$	How fast the cardiomyocytes are contracting. - Indicative of the pacing of the cardiomyocyte.
Depolarization Duration Mean $\overline{T}_{DD}$	Ca^{2+} upstroke velocity. - Indicative of the duration Ca^{2+} depolarization channels stay open.
Repolarization 30%, 60%, 90% Duration Mean $\overline{T}_{R30/R60/R90}$	Ca^{2+} decay kinetics. - Indicative of the efficiency of the Ca^{2+} repolarization channels, Ca^{2+}-ATPase (SERCA) and Na^{+}-Ca^{2+} exchanger (NCX).
Calcium Transient Duration Mean $\overline{T}_{CTD}$	Entire duration that Ca^{2+} is residing in the cytosol during a contraction.
Calcium Transient Duration normalized to Beat to Beat duration Mean $\overline{T}_{CTD\ NB}$	Proportion of the duration between contractions that the cardiomyocyte spends depolarized. - Larger ratios indicate shorter refractory periods between Ca^{2+} releases
Depolarization Duration normalized to Calcium Transient Duration Mean $\overline{T}_{Depolarization\ NCTD}$	Proportion of a calcium transient corresponding to the depolarization phase. - Larger ratios indicate that a larger proportion of the calcium transient duration is spent depolarizing as opposed to repolarizing.
Repolarization Duration 30% normalized to 90% repolarization, Mean $\overline{T}_{Repolarization30\ NR90}$	Indicative of Ca^{2+} repolarization channels kinetics - Larger ratios indicate slower speed of Ca^{2+} repolarization channels opening, resulting in a steeper sigmoidal function of the Ca^{2+} decay.

Table S4: Related to Results

Theorized molecular explanations for the variation in each Ca^{2+} handling parameter of an individual cardiomyocyte

Parameter (Variations)	**Biological Meaning**
Beat to Beat Relative Standard Deviation $\mathbf{RSD}(T_{BTB})$	Variation in the time difference between every contraction. - Indicative of the steady state of Ca^{2+} flow.
Depolarization Duration Relative Standard Deviation $\mathbf{RSD}(T_{DD})$	Variation in the Ca^{2+} upstroke velocity. - Indicative of the steady state of Ca^{2+} flow and the stability of Ca^{2+} depolarization channels.
Repolarization 90% Duration Relative Standard Deviation $\mathbf{RSD}(T_{R90})$	Variation in the Ca^{2+} decay kinetics. - Indicative of the steady state of Ca^{2+} flow with respect to Ca^{2+} decay kinetics.
Calcium Transient Duration Relative Standard Deviation $\mathbf{RSD}(T_{CTD})$	Variation of the entire duration that Ca^{2+} is residing in the cytosol during a contraction. - Indicative of the steady state of Ca^{2+} flow considering both Ca^{2+} upstroke and decay.
Calcium Transient Duration normalized to Beat to Beat duration Standard Deviation $\mathbf{SD}(T_{CTD\ NB})$	Variation in the proportion of the duration between contractions that the cardiomyocyte spends depolarized. - Indicative of the steady state of Ca^{2+} flow considering Ca^{2+} refractory periods.
Depolarization Duration normalized to Calcium Transient Duration Standard Deviation $\mathbf{SD}(T_{Depolarization\ NCTD})$	Variation in the proportion of the Ca^{2+} transient duration corresponding to the depolarization phase. - Indicative of the steady state of Ca^{2+} flow considering both Ca^{2+} upstroke and decay.
Repolarization Duration 30% normalized to 90% repolarization $\mathbf{SD}(T_{Repolarization\ NR90})$	Variation in Ca^{2+} repolarization channel kinetics - Indicative of the steady state of Ca^{2+} flow with respect to Ca^{2+} decay kinetics.

Table S5: Related to Figure S3

Insertion and deletion mutagenesis regions for each of the alleles in the three AnkB mutants used in this manuscript

Cell Line		Mutation Region	Insertion	Deletion
Parental H7 WT		GTCATGCACTGTTGAAGTAC		
Ank1	Allele 1	GTCATGCACTGTTGA*AGTAC	GAGCAGAGGGT (9bp)	AGTACTGGC (11bp)
	Allele 2	GTCATGCACTGTTGAAGT*AC		ACTGGCTAGAGAG (13bp)
Ank2	Allele 1	GTCATGCACTGT*TGAAGTAC		TGAAGTACTGGCTAGAGAGGGATG GGAAACATGCTACAGGT (41bp)
	Allele 2	GTCATGCACTGTTGAAG*TAC	ACTAG (5bp)	
Ank3	Allele 1	GTCA*TGCACTGTTGAAGTAC		TGCACTGTTGAAGTAC TGGCTAGAGA (26bp)
	Allele 2	GTCATGCAC*TGTTGAAGTAC		TGTTGAAGTAC (11bp)

*Marks the beginning of the mutagenesis
GT in Ank2 Allele2 deletion is part of the intronic region

Table S6: Related to Experimental Procedures

List of DNA oligonucleotides used in this manuscript

DNA Oligonucleotide	Usage	5' to 3' Sequence
POU5F1 Forward Primer	qPCR (Fig. S2A)	TCAGCCAAACGACCATCTGCC
POU5F1 Reverse Primer		TTCTCTTTCGGGCCTGCACG
SOX2 Forward Primer		ATGCCTTCATGGTGTGGTCCC
SOX2 Reverse Primer		TCCGGGTGCTCCTTCATGTG
NANOG Forward Primer		AATGGTGTGACGCAGAAGGCC
NANOG Reverse Primer		TTGGAAGGTTCCCAGTCGGG
ACTB Forward Primer		CCCATCGAGCATGGTATCATC
ACTB Reverse Primer		AGAAGCATACAGGGATAGCACT
TNNT2 Forward Primer	qPCR (Fig. S4C)	CAGAGCGGAAAAGTGGGAAGA
TNNT2 Reverse Primer		TCGTTGATCCTGTTTCGGAGA
GCaMP6s amplification Forward Primer	Cloning CMV-GCaMP6s (Fig. S1A)	TAGTTAGTCGACATGGGTTCTCATCATCA
GCaMP6s amplification Reverse Primer		ATATTAACGCGTTCACTTCGCTGTCATC
AAVS1 gRNA Forward strand	Cloning CMV-GCaMP6s (Fig. S1A)	CACCG**GGGGCCACTAGGGACAGGAT**
AAVS1 gRNA Reverse strand		AAAC**ATCCTGTCCCTAGTGGCCCC**C
AAVS1 flanking Forward Primer	Genotyping Validation (Fig. S1D)	ATCCTCTCTGGCTCCATCGTA
AAVS1 flanking Reverse Primer		GCCATTGTCACTTTGCGCT
GCaMP6s qgPCR Forward Primer	Genotyping Validation qgPCR (Fig. S1G); Early/Late Passage qPCR (Fig. S2C)	ACCATGGTCGACTCATCACG
GCaMP6s qgPCR Reverse Primer		TTCTTCTGCTTGTCGGCCTT
RELL1 Forward Primer	qgPCR reference gene (Fig. S1G)	TGCTTGCTCAGAAGGAGCTT
RELL1 Reverse Primer		TGGGTTCAGGAACAGAGACA
FragP1 Forward Primer	Plasmid fragment insertion PCR screen (Fig. S1F)	TCACTGGCCGTCGTTTTACA
FragP1 Reverse Primer		TCCCTTGTCCAGATAGCCCA
FragP2 Forward Primer		TGCCTGCTTGCCGAATATCA
FragP2 Reverse Primer		ATCTACACGACGGGGAGTCA
FragP3 Forward Primer		GGACAGGTATCCGGTAAGCG
FragP3 Reverse Primer		CCTGGGGTGCCTAATGAGTG
ANK2 gRNA Forward strand	ANK2 mutagenesis (Fig S3)	CACCG**GTCATGCACTGTTGAAGTAC**
ANK2 gRNA Reverse strand		AAAC**GTACTTCAACAGTGCATGAC**C
ANK2 sequencing Forward Primer	ANK2 Sequencing (Fig S3; Table S5)	TTTTGGAATCAAATGGGCCTG
ANK2 sequencing Reverse Primer		ACTGCAGATTAATGGCATTTGCT
LMNA sequencing Forward Primer	LMNA Sequencing (Fig S4A)	CTCCCACTGCAGCAGCTC
LMNA sequencing Reverse Primer		GTGACCAGATTGTCCCCGAA

*gRNA target sequences are in **bold**

Supplemental Experimental Procedures

Maintenance of hPSCs

All hPSC lines used in this study were maintained feeder-free on Matrigel® matrix coated culture plates using StemMACS™ iPS-Brew XF containing 1X iPS-Brew XF supplement (Miltenyi Biotec, Germany) and 1% Penicillin/Streptomycin (Gibco, U.S.A.). Cells were maintained at 37°C under a humidified atmosphere with 5% CO_2. Passaging was done at 80-90% confluence using 1mg/ml Collagenase IV (Gibco, U.S.A). All experiments were performed with mycoplasma-free cells. H7 ESCs and BJ iPSCs were purchased from WiCell Research Institute. HGPS fibroblasts were purchased from NIA Aging tissue bank and reprogrammed into the HGPS line.

Transfection and clonal isolation of hPSCs

In preparation for transfection, hPSCs were dissociated using Accutase (Nacalai Tesque) at 37°C for 3 minutes and 250K cells were seeded overnight on single wells of a 6 well plate. The next day, plasmids were transfected into the seeded hPSCs using Lipofectamine™ Stem transfection reagent (Invitrogen™) at plasmid size dependent concentrations. For clonal isolation, hPSCs were dissociated using Accutase and resuspended in Phosphate Buffered Saline (PBS) containing 0.5% Fetal Bovine Serum (FBS), 1% Bovine Serum Albumin (BSA), 1% Penicillin/Streptomycin (Gibco, U.S.A.) and 5μM Y27632 (Miltenyi Biotec, Germany) and sorted into single wells using the LSR II (BD Biosciences, U.S.A).

GCaMP6s was stably knocked into each hPSC cell line using a Cas9 homology directed repair protocol described previously with slight modifications (Jiang et al., 2018; Ran et al., 2013). *AAVS1* targeting gRNA was cloned into pSPCas9(BB)-2A-GFP (Addgene #48138; a gift from Feng Zhang). GCaMP6s donor plasmid was generated by inserting the GCaMP6s PCR amplicon from pGP-CMV-GCaMP6s (Addgene #40753; a gift from Douglas Kim & GENIE Project) into AAVS1-CAG-hrGFP (Addgene #52344; a gift from Su-Chun Zhang), replacing GFP. The optimized plasmid amounts used were AAVS1 gRNA plasmid containing Cas9 (0.6μg) and GCaMP6s donor plasmid (3.6μg) transfected with 10μL of Lipofectamine™ Stem in 2mL of iPS-Brew. Two days after transfection, cells were first selected using 1μg/ml puromycin for two days, and thereafter live cell sorted into single cells for clonal isolation.

A similar Cas9 directed mutagenesis was carried out to obtain the AnkB truncation clones (Ran *et al.*, 2013). *ANKB* targeting gRNA was cloned into pU6-(BbsI)_CBh-Cas9-T2A-mCherry (Addgene #64324; a gift from Ralf Kuehn). Disruption of the *ANKB* locus was first identified by PCR genotyping and confirmed using Sanger Sequencing. DNA oligonucleotide primers and gRNA sequences are listed in table S6. The optimized plasmid amount used for the ANKB gRNA plasmid containing Cas9 and mCherry was 0.7μg, transfected with 10μL of Lipofectamine™ Stem in 2mL of iPS-Brew. One day after transfection, the cells were live cell sorted, and cells positive for mCherry expression were sorted clonally into a 96 well plate for clonal expansion. Single clones were expanded until sufficient cells can be harvested for gDNA purification and downstream analysis. Disruption of the ANKB locus was first identified by PCR genotyping and confirmed using Sanger Sequencing. DNA oligonucleotide primers and gRNA sequences are listed in table S6.

Cardiomyocyte differentiation, selection and maturation

For differentiation, hPSCs were passaged in single cells using Accutase (Nacalai Tesque) and subjected to the previously established small molecule based GiWi cardiomyocyte differentiation protocol (Lian et al., 2013). At Day 7, the media was replaced with RPMI1640 (HyClone) containing 1X B27 with insulin supplement (Miltenyi Biotec) for maturation and refreshed every 2 days. At Day 14, the glucose level in the media was slowly reduced to 0% by Day 21, and the media was replaced with RPMI1640, 0% Glucose (HyClone), containing 1X B27 with insulin supplement, 100 μM Oleic Acid, 50 μM Palmitic Acid and 10mM Galactose to facilitate the metabolic maturation and selection of the cardiomyocytes to β-oxidation as described previously (Correia et al., 2017). On day 28, hPSC-CMs were used for Ca^{2+} imaging directly. For the drug-induced arrhythmogenesis dataset, BJ-CMs were treated with either DMSO as a vehicular control, 10μM or 40μM E4031 for 2 hours before Ca^{2+} imaging.

RNA extraction, reverse transcription and quantitative PCR

Cells were harvested in TRIzol (Invitrogen, U.S.A) and RNA was purified using Chloroform (Kanto Chemical, Japan) phase separation. 1µg of purified RNA was reverse transcribed using High-Capacity cDNA Reverse Transcription Kit (Applied Biosystems, U.S.A.). Quantitative PCR was performed using FAST SYBR Green Mix (Applied Biosystems, U.S.A.), 0.3µM of specific primers (Table S6) and ~5ng of cDNA. $\Delta\Delta C_T$-based relative quantification method was adopted for qPCR analysis using the QuantStudio 5 384-well Block Real-Time PCR system (Applied Biosystems, U.S.A.). The threshold cycle was determined to be 40. Data is presented as fold-change where CT values were normalised to *ACTB*.

Genomic DNA extraction, standard PCR and quantitative genotyping PCR

Cells were harvested using Accutase (Nacalai Tesque) and the genomic DNA was purified using Wizard® Genomic DNA Purification Kit (Promega) following manufacturer protocols. Standard PCR amplification was done using GoTaq® Green Master Mix (Promega). Quantitative genotyping PCR was carried out by adapting the protocol provided in (Simkin et al., 2022). Briefly, 1µg of genomic DNA was digested to completion with EcoRI (NEB) and heat-inactivated at 65°C. ~10 ng of digested gDNA was loaded with 0.5µM of qgPCR primers into the FAST SYBR Green Mix (Applied Biosystems, U.S.A.) for quantitative PCR run. $\Delta\Delta C_T$-based relative quantification method was adopted for qgPCR analysis using the QuantStudio 5 384-well Block Real-Time PCR system (Applied Biosystems, U.S.A.). The threshold cycle was determined to be 40. ΔCT values were normalized to *RELL2* as a stable housekeeping gene corresponding to 2 allele copies.

Protein extraction and western blot

Cells were harvested in RIPA buffer (ThermoScientific, U.S.A.) and protein quantification was carried out using Pierce™ BCA Protein Assay Kit (Thermo Scientific, U.S.A.). 30ng of protein lysates were resolved in 8% SDS-PAGE gels in Tris-Glycine-SDS buffer before being transferred to PVDF membranes (Bio-Rad, U.S.A) for probing with specific antibodies and imaging using Clarity™ ECL Western Substrate (Bio-Rad, U.S.A). Primary antibodies used are as follows: anti-AnkB mouse (1:200; Abcam; ab131419), anti-LMNA/C mouse (1:500; Abcam; ab40567), anti-β-actin mouse (1:1000; Cell Signaling Technology, 3700S), anti-GAPDH rabbit (1:2500; Abcam; ab9485). Secondary antibodies conjugated with horseradish peroxidase (1:1000; Santa Cruz Biotechnology, U.S.A; sc-516102) were used.

Fluorescent cytometric analysis

hPSC-CMs were dissociated in a similar manner to hPSCs described above. CMs were stained with anti-human CD172a/b (SIRPα/β) conjugated antibody (1:300; Biolegend; #323808) for 1 hour in PBS containing 1% FBS. The cells were washed thoroughly and resuspended in PBS containing 0.5% FBS and 1% BSA for flow cytometric analysis performed using LSR II (BD Biosciences, U.S.A.).

Statistical analysis

All statistical analysis were performed using R. Students *t* test was used to compare quantitative gene expression results and all parameters across treatment groups in each ML dataset. All tests were two-tailed, and $P < 0.05$ were considered significant.

Supplemental References

Correia, C., Koshkin, A., Duarte, P., Hu, D., Teixeira, A., Domian, I., Serra, M., and Alves, P.M. (2017). Distinct carbon sources affect structural and functional maturation of cardiomyocytes derived from human pluripotent stem cells. Scientific Reports *7*, 8590. 10.1038/s41598-017-08713-4.

Jiang, Y., Zhou, Y., Bao, X., Chen, C., Randolph, L.N., Du, J., and Lian, X.L. (2018). An Ultrasensitive Calcium Reporter System via CRISPR-Cas9-Mediated Genome Editing in Human Pluripotent Stem Cells. iScience *9*, 27-35. 10.1016/j.isci.2018.10.007.

Lian, X., Zhang, J., Azarin, S.M., Zhu, K., Hazeltine, L.B., Bao, X., Hsiao, C., Kamp, T.J., and Palecek, S.P. (2013). Directed cardiomyocyte differentiation from human pluripotent stem cells by modulating Wnt/β-catenin signaling under fully defined conditions. Nat Protoc *8*, 162-175. 10.1038/nprot.2012.150.

Ran, F.A., Hsu, P.D., Wright, J., Agarwala, V., Scott, D.A., and Zhang, F. (2013). Genome engineering using the CRISPR-Cas9 system. Nat Protoc *8*, 2281-2308. 10.1038/nprot.2013.143.

Simkin, D., Papakis, V., Bustos, B.I., Ambrosi, C.M., Ryan, S.J., Baru, V., Williams, L.A., Dempsey, G.T., McManus, O.B., Landers, J.E., et al. (2022). Homozygous might be hemizygous: CRISPR/Cas9 editing in iPSCs results in detrimental on-target defects that escape standard quality controls. Stem Cell Reports *17*, 993-1008. https://doi.org/10.1016/j.stemcr.2022.02.008.